IOP Conf. Series: Materials Science and Engineering **47** (2013) 012025 doi:10.1088/1757-899X/47/1/012025

Investigations on optical, structural and thermal properties of phosphate glasses containing terbium ions

M Elisa[1], B A Sava[1], I C Vasiliu[1], R C C Monteiro[2], C R Iordanescu[1], I D Feraru[1], L Ghervase[1], C Tanaselia[3], M Senila[3], B Abraham[3]

[1]Department of Optospintronics, National Institute of R & D for Optoelectronics INOE 2000, 77125 Magurele, Romania
[2]CENIMAT/I3N, Department of Materials Sciences, Faculty of Sciences and Technology,
Universidade Nova de Lisboa, 2825-516 Caparica, Portugal
[3]The Research Institute for Analytical Instrumentation, 400293 Cluj-Napoca

E-mail: icvasiliu@inoe.inoe.ro

Abstract. Aluminophosphate glasses belonging to the Li_2O–BaO–Al_2O_3–La_2O_3–P_2O_5 system doped with Tb^{3+} were prepared and investigated. Methods as Induced Coupled Plasma-Mass Spectrometry (ICP-MS), Induced Coupled Plasma-Atomic Emission Spectroscopy (ICP-AES) and X-ray diffraction (XRD) have been used to establish the elemental composition of these vitreous materials. The influence of the Tb^{3+} ions on the optical properties of the phosphate glasses has been investigated in relation with the structural characteristics of the vitreous matrix. The optical behavior has been studied by ultra-violet–visible (UV–Vis) spectroscopy, revealing electronic transitions specific for terbium ions. Fluorescence spectroscopy measurements have been performed by excitation in the UV and visible domains (377 nm and 488 nm) which resulted in the most significant fluorescence peaks in the Vis domain (540 and 547 nm). Structural information via vibration modes were provided by Fourier Transform Infrared (FTIR) absorption spectra in the 400–4000 cm^{-1} range. Absorption peaks specific for the vitreous phosphate matrix were put in evidence as P-O-P symmetrical and asymmetrical stretching vibration modes, P-O-P bend, PO_2- symmetrical and asymmetrical stretching vibration modes, P=O stretching vibration mode as well as P-O-H water absorbance. Raman spectra acquired in the 100–4000 cm^{-1} range by 488, 514 and 633 nm laser excitation sources disclosed peaks also specific for the phosphate matrix, proving the role of phosphorous oxide as a vitreous network former. Differential Scanning Calorimetry and Thermogravimetric Analysis (DSC-TGA) provided information regarding the phase transformations that took place during the heating process and the associated thermal effects.

1. Introduction

Phosphate glasses are attractive for different applications due to their interesting properties among which the very high solubility for rare-earth ions. The electronic energy levels of the rare-earth ions essentially determine the lasing characteristics of rare-earth doped materials and are considerably influenced by the presence of other ions in their vicinity [1-4].

Rare-earth doped glasses have generated a great deal of interest as potential materials particularly in the glasses-based laser technology. For example, rare-earth ion Tb^{3+} - doped $ZnO–B_2O_3–SiO_2$ glasses as a function of terbium ion concentration was studied to optimize the luminescent centers in the glass system for a better fluorescence performance [5].

The external quantum efficiency of phosphate glass containing 10 mol% Tb^{3+} was measured to be 78%. The large value of ΔT (T_x - T_g) of the glasses was about 340 °C, which guarantees the thermal stability of the glasses against crystallization during the fiber drawing process, and Tb^{3+} - doped phosphate glass fibers have been successfully drawn [6].

It was developed a new concept of energy transfer sensitization based on nearly resonant energy migration through a rare earth ion subsystem in the glass matrix followed by a single-step transfer to the Ce^{3+} (Tb^{3+}) emission centers. In more detail, Gd^{3+} ions at sufficiently high concentration enable effective energy migration in the phosphate and silicate-based glass matrices followed by a single-step energy transfer towards emission centers created by Ce^{3+} or Tb^{3+} doping [7].

Also, rare-earth-doped glasses have been investigated intensively regarding their magnetic properties and Faraday effects, Tb-doped glasses having the largest Verdet constant [8,9].

Studies of the optical behavior of terbium-doped sol–gel glasses materials provide information about the interactions between the dopants and the surrounding matrix, as well as insight into long-range interactions and energy transfer between dopant impurities [10].

The present work is based on the results of a study that aims at improving the homogeneity of the aluminophosphate glasses doped with terbium ions and hence the optical properties, by using a wet non-conventional method of synthesis [11]. The prepared glasses are used in optical sensors based on fluorescence in the visible domain.

2. Experimental

In this work Tb^{3+}- doped $Li_2O–BaO–Al_2O_3–La_2O_3–P_2O_5$ glasses have been prepared using Li_2CO_3, $BaCO_3$, Al_2O_3, La_2O_3, H_3PO_4 and Tb_2O_3 as analytical grade reagents. The reagents are introduced in H_3PO_4 solution at the very beginning of the starting process, under continuous stirring.

Major element such as phosphorous followed by lithium, barium, and aluminium have been analyzed by Induced Coupled Plasma – Atomic Emission Spectroscopy (ICP-AES), model Perkin-Elmer Optima 530DV, plasma power 1350 W, concentric nebulizer Meinhardt, argon flow 1.15 ml/min. There were made five measurements with the relative standard deviation (RSD) < 2% and the detection resolution 10 µg/L.

Terbium ions has been analyzed by Induced Coupled Plasma – Mass Spectrometry (ICP-MS), model Perkin Elmer Elan DRC II, equipped with a quadrupol, plasma power 1250 W, concentric nebulizer Meinhardt, argon flow 0.86 ml/min. There were made five measurements with the relative standard deviation (RSD) < 2% and the detection resolution 1 µg/L.

The X-ray diffraction patterns were recorded on a Rigaku Dmax III-C 3kW diffractometer (Rigaku Corporation, Tokyo, Japan), using CuKα radiation at 40 kV and 30 mA settings in the 2θ range from 20º to 60º, an acquisition time of 1 s and 2θ increment of 0.04º. The crystalline phases were identified by comparing the peak positions and intensities with those listed in the software standard files (ICDD, Newtown Square, PA, USA). XRD analysis was performed in the glass sample after heat treatment. Powder glass sample was compacted, by pressing in a mold, and the compacts were treated in an electrical furnace at a heating rate of 5 ºC/min up to a selected temperature and then the furnace was switched off and the sample allowed to cool inside the furnace. Temperature for treatment (600 and 680 ºC) was selected taking into account the DTA results.

The optical behavior has been studied by ultra-violet–visible (UV–Vis) spectroscopy by means of Perkin Elmer Lambda 1050 spectrophotometer, in the 300-700 nm range.

Fluorescence spectroscopy measurements were made with an Edinburgh Instruments FLS 920 Spectrofluorimeter, equipped with a 450 W Xenon lamp and double monochromator, both for excitation and emission. The spectra were recorded in the UV and visible domains (377 nm and 488 nm) with 1 nm step, integration time 0.2 s.

FTIR spectra were recorded with a Perkin Elmer Spectrophotometer-Spectrum 100, provided with UATR accessory (Universal Attenuated Total Reflectance) in the range 400-4000 cm^{-1}. The measurement error is ± 0.1% and the number of scans 32.

Raman spectra were collected by means of LabRAM HR 800 UV–VIS-NIR Horiba Jobin-Yvon system, at room temperature, acquired in the 100-4000 cm^{-1} range. The samples were excited by 514 nm laser line, focused on the surface sample with a confocal microscope, using an objective magnification x100, 1 μm^2 laser spot size, 2.6 mW laser power on the surface sample, 0.5 to 1 cm^{-1} resolution and 1800 grating/mm diffraction network.

Information regarding the phase transformations that took place during the heating process and the associated thermal effects were provided by Differential Scanning Calorimetry and Thermogravimetric Analysis (DSC-TGA). The tests were performed in thermal analysis equipment STA PT 1600, Linseis, Germany. Glass powder sample was used, obtained by hand grinding the glass in an agate mortar until a powder with particle size < 65 µm was obtained. Previously to the DSC-TG characterization, the powder has been dried at 120 ºC for 3 h. The sample was heated in static air, at a constant heating rate (5 ºC/min) from room temperature up to a maximum temperature of 800 ºC. The sample was heated inside alumina crucible, and an empty alumina crucible was used as reference.

3. Results and discussions

The chemical composition of Tb-doped glass determined by ICP-MS and ICP-AES analysis is presented in Table 1.

Table 1. ICP-MS and ICP-AES results of Tb-doped glass

	Li_2O	BaO	Al_2O_3	La_2O_3	P_2O_5	Tb_2O_3
ICP-MS (AES)	5.65	0.51	7.46	0.02	86.30	0.05

XRD patterns for the Tb-doped glass treated at 600 ºC (for 1 hour) and at 680 ºC are shown in figure 1. The peaks corresponding to the different phases are identified. It can be seen that for 680 ºC, the predominant phase is $Al(PO_3)_3$. From peaks identification, $AlPO_4$ appears to be present as different crystallographic forms (eg. orthorhombic and hexagonal). At 600 ºC, the sample is still amorphous.

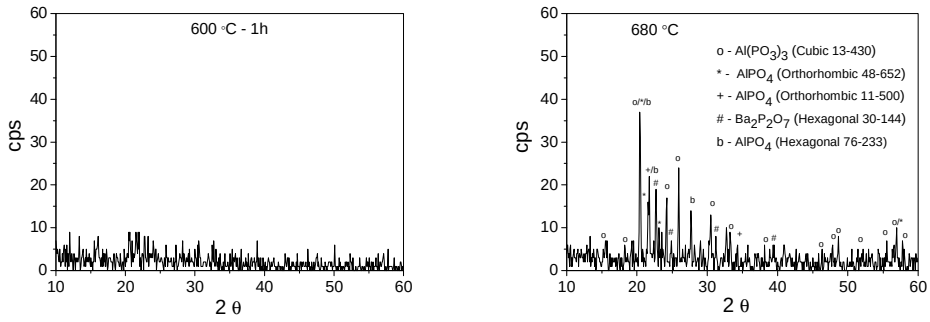

a) b)

Figure 1. XRD patterns for Tb-doped glass treated at a) 610 ºC, and b) at 680 ºC

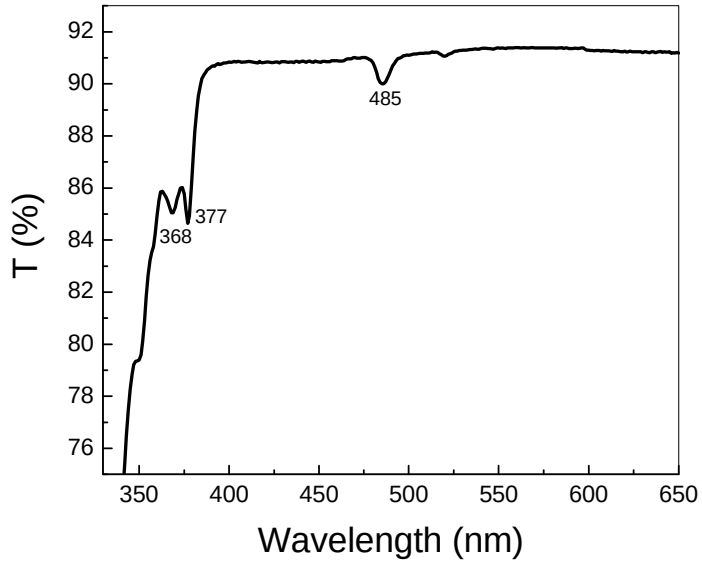

Figure 2. UV-VIS transmission spectrum of Tb^{3+} - doped $Li_2O–BaO–Al_2O_3–La_2O_3–P_2O_5$ glass

UV-VIS investigations presented in figure 2, disclose several absorption bands 368 nm, 377 nm and 485 nm, attributed to electronic transitions specific for terbium ions. The two intense peaks centered at 377 nm and 485 nm were used as excitation wavelengths to generate fluorescence emission.

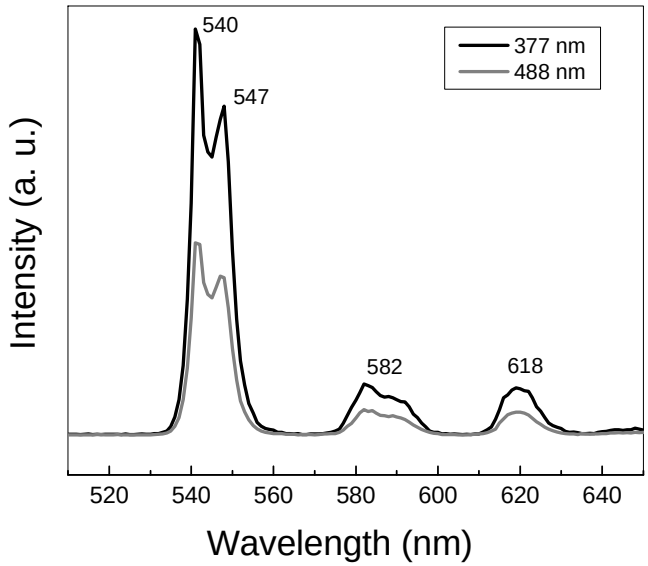

Figure 3. Fluorescence spectra of Tb^{3+} - doped $Li_2O–BaO–Al_2O_3–La_2O_3–P_2O_5$ glass excited with 377 nm and 488 nm

The fluorescence spectra of Tb^{3+} - doped glass samples are presented in the figure 3. Tb^{3+} have fluorescence signals in the visible range, 540 nm ($^5D_4 \rightarrow {}^7F_6$) and 547 nm ($^5D_4 \rightarrow {}^7F_5$) obtained by 377 and 488 nm excitation, the more intense peak being centered at 540 nm.

Also, it is to be noticed the presence of two other small peaks at 582 nm ($^5D_4 \rightarrow {}^7F_4$) and 618 nm ($^5D_4 \rightarrow {}^7F_3$).

The FTIR absorption spectrum of terbium-doped and undoped glass samples (figure 4) reveals peaks specific for phosphate vitreous network that emphasize the vitreous network-forming role of P_2O_5. The FTIR spectrum of Tb-doped glass shows the presence of absorption bands at ~770, 895, 1075, 1255, cm^{-1}, corresponding to the vibration modes as presented in the table 2. Thus, the absorption bands situated at ~770 cm^{-1} and at ~ 895 cm^{-1} characteristic for ν_s (P–O–P) Q^2 and Q^1 structural units and ν_{as} P–O–P Q^2 and Q^1 structural units, respectively, slowly decrease in intensity in the case of doped glass , due to some broken P–O linkages [12]. The intensities of the bands around 1075 cm^{-1} corresponding to ν_s $(PO_4)^{3-}$ in Q^0 units do not decrease in intensity as a consequence of stronger bonds that cannot be broken. The band at about 1255 cm^{-1} attributed to ν_{as} (PO_2) in Q^2 units was modified in intensity in the case of Tb-doped glass.

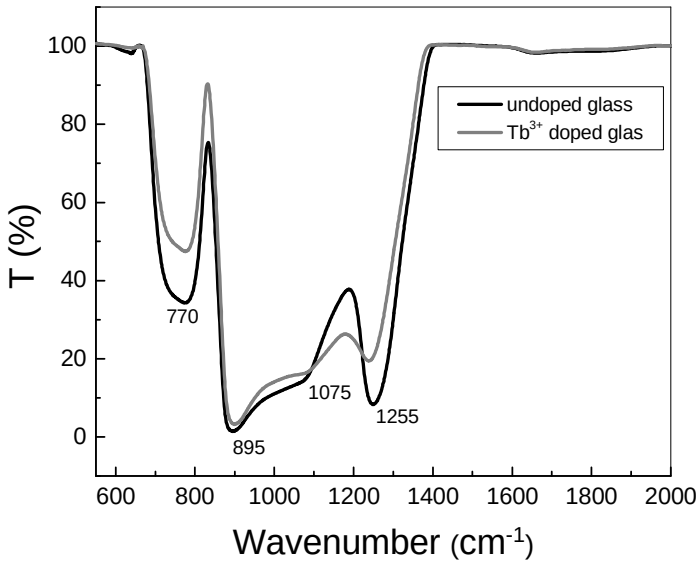

Figure 4. FTIR spectra of undoped and Tb^{3+} doped $Li_2O–BaO–Al_2O_3–La_2O_3–P_2O_5$ glasses

The figure 5 presents the Raman spectra of Tb^{3+} -doped and undoped glass samples. The presence of the following main peaks was noticed at 355, 705, 979 and 1194 cm^{-1} (table 2). Thus, we attributed, in agreement with literature data [12-14] the peak located at 355 cm^{-1} to transverse-optical (TO) Raman mode vibration of P-O-P bonds, the peak at 705 cm^{-1} to ν_s (P-O-P) Q^2 and Q^1 structural units, the peaks located around 979 and 1194 cm^{-1} to ν_s $(PO_4)^{3-}$ in Q^0 units and ν_s (PO_2) in Q^2 units, respectively.

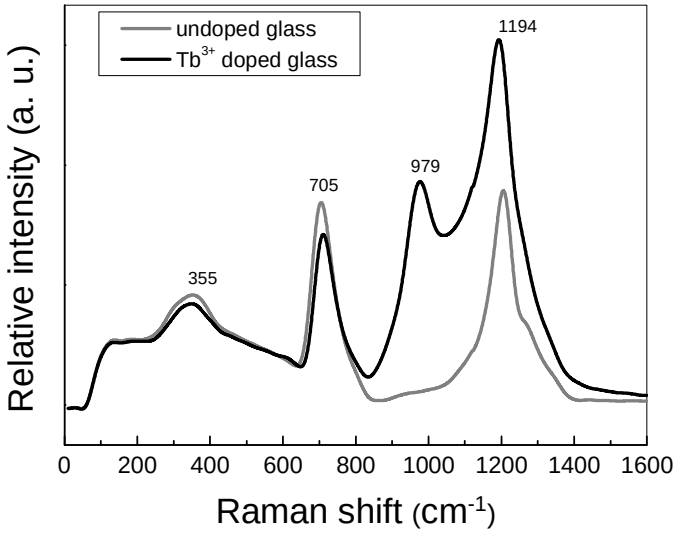

Figure 5. Raman spectra of undoped and Tb^{3+} doped $Li_2O–BaO–Al_2O_3–La_2O_3–P_2O_5$ glasses

Table 2. Bands assignment in Raman and FTIR spectra of Tb^{3+} doped and undoped $Li_2O–BaO–Al_2O_3–La_2O_3–P_2O_5$ glasses (δ = bending vibration mode; ν = stretching vibration mode)

Wavenumber (cm^{-1})	Raman shift	FTIR
355	δ (O-P-O)	
705	ν_s (P-O-P) Q^2 and Q^1 structural units	
770		ν_s (P-O-P) Q^2 and Q^1 structural units
895		ν_{as} P–O–P Q^2 and Q^1 structural units
979	$\nu_s (PO_4)^{3-}$ in Q^0 units	
1075		$\nu_s (PO_4)^{3-}$ in Q^0 units
1194	ν_s (PO_2) in Q^2 units	
1255		ν_{as} (PO_2) in Q^2 units

From the analysis of the DSC curve, characteristic temperatures associated to structural changes in the glass sample were determined. Generally, the heat flow curve shows an endothermic effect, corresponding to the glass transition temperature (T_g), and a sharp exothermic effect, corresponding to the crystallization of the glass, with a maximum at temperature named as T_p.

TG curve revealed no weight loss during the heating process, that is, the mass change (dM) curve does not have significant modifications during the heat treatment, as it would be expected for glass samples.

Figure 6 shows the DSC-TG curves obtained at a heating rate of 5 ºC/min for the phosphate glass doped with Tb. Heat flow curve for the investigated glass present an endothermic effect at a temperature in the range 430 ºC–460 ºC, corresponding to the glass transition temperature (T_g) at 461 ºC, and an exothermic effect with a maximum at a temperature T_p at 549 ºC.

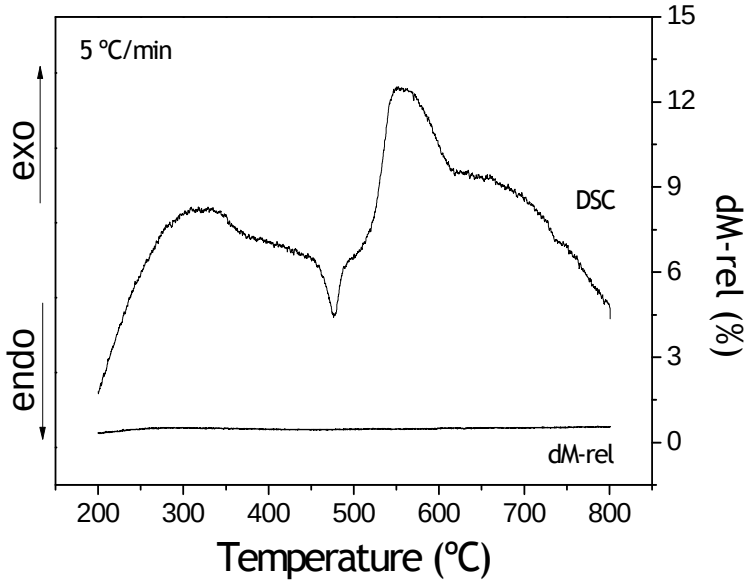

Figure 6. DSC-TG curves obtained at a heating rate of 5 ºC/min for the phosphate glass doped with Tb^{3+}

4. Conclusions

Tb-doped aluminophosphate glass prepared by a non-conventional melting-quenching method was investigated by optical spectroscopy methods. The UV–VIS transmission spectrum is strongly dependent on the doping ions nature, revealing peaks due to the electronic transition between the inner orbitals of the Tb ion. Fluorescence spectroscopy measurements performed by excitation with 377 nm and 488 nm resulted in the most significant fluorescence peaks in the Vis domain (540 and 547 nm), specific for the electronic transitions from the excited states to the ground state of the Tb ions. IR absorption spectra as well as the Raman spectra revealed structural units of the glass matrix, proving the role of phosphorus as a vitreous network former. The vitreous transition (T_g) and crystallization (T_p) temperatures were put in evidence during the glass heating.

Acknowledgements

The authors are grateful to UEFISCDI (Executive Unity for Financing of Higher Education, Research and Innovation), Romania for the financial support in the frame of 7-031/2011 MNT- ERA.NET contract and 168/2012 Partnership Program contract and to the Portuguese Foundation for Science and Technology for financing ERA-MNT/001/2010 and PEst-C/CTM/LA0025/2011 projects.

References

[1] Reisfeld R and Jorgensen C K 1976 *Phys. Rev. B13* **81**
[2] Campbell J H and Suratwala T I 2000 *J. Non-Cryst. Solids* **318** 263–264
[3] Hazarika S and Rai R 2004 *Opt. Mater.* **27** 173
[4] Goget G A, Gaumer N, Obriot J, Rammal A, Chaussedent S, Monteil A, Portales H, Chiasera A and Ferrari M 2005 *J. Non-Cryst. Solids* **351** 1754
[5] Sooraj Hussain N, Prabhakara Reddy Y and Buddhudu S 2001 *Materials Letters* **48** 303–308

[6] Zhang L, Peng M, Dong G and Qiu 2012 J *Optical Materials* **34** 1202-1207
[7] Baccaro S, Dall'Igna R, Fabeni P, Martini M, Mares J A, Meinardi F, Nikl M, Nitsch K, Pazzi G P, Polato P, Susini C, Vedda A, Zanella G and Zannoni R 2000 *Journal of Luminescence* **87-89** 673-675
[8] Berger S B, Rubinstein C B, Kurkjian C R and Treptow A W 1964 *Phys. Rev.* **133** A723-A727
[9] Rubinstein C B, Berger S B, Van Uitert L G and Bonner W A 1964 *J. Appl. Phys*. **35** 2338
[10] Silversmith A J, Boye D M, Brewer K S, Gillespie C E, Lua Y, Campbell D L 2006 *Journal of Luminescence* **121** 14–20
[11] Elisa M, Vasiliu I C, Grigorescu C E A, Grigoras B, Niciu H, Niciu D, Meghea A, Iftimie N, Giurginca M, Trodahl H J and Dalley M 2006 *Optical Materials* **28 (6-7)** 621-625
[12] Lai Y M, Liang X F, Yang S Y, Wang J X, Cao L H and Dai B 2011 *Journal of Molecular Structure* **992** 84–88
[13] Li Y, Ashton B and Jackson S D 2005 *Optics Express* **13** Issue 4 1172-1177
[14] Koo J, Bae B-S and Na H-K 1997 *Journal of Non-Crystalline Solids* **212** 173-179